



## DENGUE DYNAMICS: BAYESIAN SPATIO-TEMPORAL ANALYSIS USING INTRINSIC CONDITIONAL AUTOREGRESSIVE MODEL

Dinah Dumaguing<sup>1,2,\*</sup>, and Daisy Lou L. Polestico<sup>1,2</sup>

<sup>1</sup>Department of Mathematics and Statistics

MSU-Iligan Institute of Technology, 9200 Iligan City, Philippines

[dinah.dumaguing@g.msuiit.edu.ph](mailto:dinah.dumaguing@g.msuiit.edu.ph)

<sup>2</sup>PRISM-Center for Computational Analytics and Modeling

MSU-Iligan Institute of Technology, 9200 Iligan City, Philippines

[daisylou.polestico@g.msuiit.edu.ph](mailto:daisylou.polestico@g.msuiit.edu.ph)

Received: 4th December 2024    Revised: 22nd August 2025

### Abstract

In data-limited regions such as the Philippines, exploring socio-economic and environmental factors beyond traditional mosquito vector studies is crucial to understanding disease dynamics. This study employed a Bayesian spatio-temporal approach to model dengue transmission in Region 10, incorporating time-varying coefficients and a latent spatial effect with an Intrinsic Conditional Autoregressive (ICAR) prior. Three models were evaluated: Model 1 included only the intercept and spatial autocorrelation term, Model 2 included time-varying covariates without spatial effects, and Model 3 incorporated both time-varying coefficients and spatial effects. Model 3 outperformed the other models in disease modeling (WAIC = 24,520.7), providing clearer insights into the relationships between key covariates and dengue incidence. In Model 3, the inclusion of the spatial effect  $\phi_i$  resulted in a shift in the relationships between key covariates and dengue incidence. The relationship between CMCI and dengue cases became negative, while elevation showed a positive association. Coastal proximity also became more negatively associated with dengue risk. Model 3 revealed that few urban areas had persistent high  $\phi_i$  values, indicating that unmeasured factors continue to influence spatial variation in dengue risk. Conversely, many other municipalities showed a reduction in the magnitude of  $\phi_i$  suggesting that covariates in Model 3 better explained the spatial variation. Graphs and plots of observed and fitted values, as well as a plot of relative risk over time, demonstrated the model's performance across both time and space. The inclusion of spatial autocorrelation and time-varying effects in Model 3 improved model fit and provided a more nuanced understanding of dengue dynamics, highlighting the importance of considering both spatial and temporal components in disease modeling.

## 1 Introduction

Dengue fever remains a critical public health concern in the Philippines, especially among children, and it incurs substantial societal and economic costs [14], [5]. The growing prevalence of

---

\*Corresponding author

2020 Mathematics Subject Classification: 62H11, 62M30

Keywords and Phrases: Bayesian, spatio-temporal, time-varying coefficients, intrinsic conditional autoregressive (icar) models, dengue incidence

This research is supported by the Department of Science and Technology-Accelerated Science and Technology Human Resource Development Program (DOST-ASTHRDP)

dengue calls for advanced approaches to understanding its transmission dynamics and improving public health strategies.

A key challenge in dengue transmission modeling is the difficulty in obtaining reliable mosquito vector data. Traditional indices like the Breteau Index, often fail to consistently correlate with transmission and current sampling methods are not ideal for routine surveillance [5],[4]. These limitations emphasize the need for alternative, more accessible variables that can still offer meaningful insights into dengue dynamics. Studies have shown that environmental and socio-economic indicators, such as climate, population density and ecological factors, can effectively contribute to understanding and predicting dengue transmission [1], [18]. As a result, research has shifted from basic descriptive analyses to more complex models that integrate these variables, providing a more comprehensive understanding of the factors influencing dengue spread.

Researchers have applied Bayesian hierarchical models, particularly Conditional Autoregressive (CAR) models, to analyze dengue fever transmission, recognizing their ability to capture spatial dependencies [2]. The dynamic nature of dengue transmission further necessitates the incorporation of temporal variations to avoid biased estimates, supporting the need for spatio-temporal models [6].

Recent advancements have further refined spatio-temporal models by incorporating time-varying coefficients. Freitas et al. (2021) enhanced the ICAR models in this way, allowing for a more nuanced understanding of how covariates influence dengue transmission over time [9]. Building on these advancements, this study aims to model the dynamics of dengue transmission in Northern Mindanao using Bayesian methodologies that integrate both spatial and temporal factors, offering new insights into the drivers of the disease.

## 2 Methodology

The analysis of dengue incidence in northern Mindanao was carried out using Bayesian spatio-temporal models, implemented through the `RStan` package [21], which is the `R` interface [20] to the Stan platform. The Stan platform is a powerful tool for Bayesian inference and provides a comprehensive framework to fit complex statistical models using Markov Chain Monte Carlo (MCMC) methods, particularly Hamiltonian Monte Carlo (HMC) [22]. In this study, the primary model used to analyze dengue incidence incorporates a spatial autoregressive component using an Intrinsic Conditional Autoregressive (ICAR) model, which captures the spatial dependency between neighboring regions.

### 2.1 Study Site and Data

The study was conducted in Northern Mindanao, encompassing 93 cities and municipalities. Weekly data on dengue case counts for the years 2021 to 2022 were requested from the Department of Health's Research Unit. Geospatial data, including elevation and coastal classification, were sourced from PhilAtlas [17]. Additionally, the population density data were obtained from the 2020 Census of Population and Housing conducted by the Philippine Statistics Authority [19]. Socioeconomic data were gathered from the Cities and Municipalities Competitiveness Index (CMCI), developed by the Department of Trade and Industry [8].

### 2.2 Statistical Model

A generalized linear model (GLM) framework was employed to analyze the relationship between various covariates and the incidence of dengue cases in the region. The count of dengue cases

$Y_{i,t}$  in the neighborhood  $i$  during week  $t$  was assumed to follow a Poisson distribution, with the expected number of cases denoted as  $\mu_{i,t}$ . This setup allowed for a flexible approach to model the count data while accommodating the overdispersion commonly observed in epidemiological data.

The Poisson distribution was chosen with a logarithmic link function, ensuring that the expected number of cases remained positive and allowing the coefficients of covariates to be interpreted in terms of relative risk. The model is given by:

$$Y_{i,t} \sim \text{Poisson}(\mu_{i,t}),$$

$$\log(\mu_{i,t}) = \log(e_i) + \beta_0 + X_i' \beta_{k,t} + \phi_i,$$

where  $\log(e_i)$  is the offset term representing the expected number of dengue cases in the absence of spatial or temporal variations, computed as the total number of dengue cases divided by the population size for each neighborhood.

$$e_i = \left( \frac{\sum_{i=1}^n \sum_{t=1}^T Y_{i,t} \cdot P_i}{\sum_{i=1}^n P_i} \right) / T,$$

### 2.2.1 Spatial Modeling: Intrinsic Conditional Autoregressive Model (ICAR)

A key feature of the analysis was the inclusion of spatial autocorrelation to account for the fact that dengue incidence in one neighborhood may be influenced by the incidence in neighboring areas. Spatial autocorrelation refers to the tendency for nearby locations to exhibit similar outcomes. In the context of this study, it was hypothesized that the occurrence of dengue cases in one neighborhood could be related to the occurrence of cases in neighboring neighborhoods due to shared environmental conditions, socioeconomic factors, or movement of individuals across neighboring regions.

To capture this spatial structure, an Intrinsic Conditional Autoregressive (ICAR) model was used. The ICAR model is a type of Conditional Autoregressive (CAR) model that is commonly employed in spatial statistics for analyzing geographic data where spatial dependencies between neighboring regions need to be accounted for.

In spatial modeling, each location (or neighborhood) is assumed to have a latent spatial effect, denoted as  $\phi_i$  for neighborhood  $i$ , which captures the influence of its neighbors on the outcome of interest (in this case, dengue incidence). The ICAR model assumes that the value of  $\phi_i$  is related to the values of its neighboring locations through a linear relationship, where each neighborhood is influenced by the average of its neighbors' spatial effects.

The spatial dependence structure is represented by a neighborhood structure matrix  $w_{ij}$ , which indicates whether two neighborhoods  $i$  and  $j$  are neighbors. Specifically:

$$w_{ij} = \begin{cases} 1, & \text{if neighborhoods } i \text{ and } j \text{ share a border,} \\ 0, & \text{otherwise.} \end{cases}$$

The ICAR prior for the spatial effect  $\phi_i$  follows a conditional normal distribution whose mean is equal to the average of its neighbors and its variance is inversely proportional to the number of neighbors  $d_i$ , that is:

$$p(\phi_i | \phi_{i \sim j}) = N \left( \frac{\sum_{i \sim j} \phi_i}{d_i}, \frac{\sigma^2}{d_i} \right),$$

where  $\phi_{i \sim j}$  represents the set of neighbors of  $i$ .

## 2.2.2 Model Structures

The different structures for  $\mu_{i,t}$  listed below were explored and their respective Watanabe-Akaike information criteria (WAIC)[24] were considered.

Table 1: Spatio-Temporal ICAR Model Structures

Model 1	$\log(\mu_{i,t}) = \log(e_i) + \beta_0 + \phi_i$
Model 2	$\log(\mu_{i,t}) = \log(e_i) + \beta_0 + X_i' \beta_{k,t}$
Model 3	$\log(\mu_{i,t}) = \log(e_i) + \beta_0 + X_i' \beta_{k,t} + \phi_i$

where:

- $\mu_{i,t}$ : Expected or mean number of dengue cases in neighborhood  $i$  during week  $t$ ,
- $e_i$ : Expected number of dengue cases at neighborhood  $i$ ,
- $\beta_0$ : Intercept,
- $\phi_i$ : Spatial autocorrelation parameter for location  $i$ ,
- $X_i'$ : Vector of  $k$  covariates,
- $\beta_{k,t}$ : Coefficient of covariate  $k$  in week  $t$ .

The progression from Model 1 to Model 3 allows for a systematic evaluation of the contributions of different components to dengue incidence. Model 1 serves as a baseline, accounting solely for spatial heterogeneity through the inclusion of the spatial effect  $\phi_i$ . This enables the assessment of whether spatial autocorrelation alone can capture patterns in dengue distribution, potentially driven by unobserved spatially structured factors.

Model 2 offers an alternative to the baseline by introducing time-varying covariates, thereby allowing for the evaluation of the influence of observed risk factors—such as elevation, CMCI scores and geographic classification (coastal or landlocked)—on dengue incidence. This formulation assumes independence across space and time, attributing changes in incidence solely to covariate effects.

Model 3 integrates both observed covariates and latent spatial effects, allowing for a more comprehensive model of disease risk. By incorporating  $\phi_i$ , this model accounts for spatially structured residual variation that may not be fully explained by the covariates. This is particularly useful in epidemiological modeling where data may be limited or covariates may not capture all local risk factors.

## 2.2.3 Model Fitting and Validation

For model fitting, the RStan package's `stan` function [21] was used to implement the Bayesian framework. Four Markov Chain Monte Carlo (MCMC) chains were run with 10,000 iterations, including a warm-up phase of 5,000 iterations. The convergence of the chains was assessed using the Gelman-Rubin statistic ( $\hat{R}$ ), which indicates whether the chains have sufficiently mixed and converged to the target distribution. The model fit was assessed by using the Watanabe-Akaike Information Criterion (WAIC) [24], a measure that balances model complexity and goodness of fit. In addition, the predictive performance of the model was validated by comparing the predicted dengue case counts to the observed data, ensuring that the model provided an accurate representation of the actual data.

### 3 Results and Discussion

The time series plot in Figure 1 presents the weekly number of dengue cases spanning January 2021 to December 2022 in Region 10. Early 2021 showed stable case counts of 70–100 cases weekly, followed by dips and spikes, including a notable increase in mid-June to late July 2021, peaking at 122 cases. A surge occurred from late September to mid-November, reaching 249 cases by year-end.

In 2022, case counts fluctuated, with a pronounced peak between mid-May and early August, exceeding 250 cases weekly and peaking at 352 cases in early July.

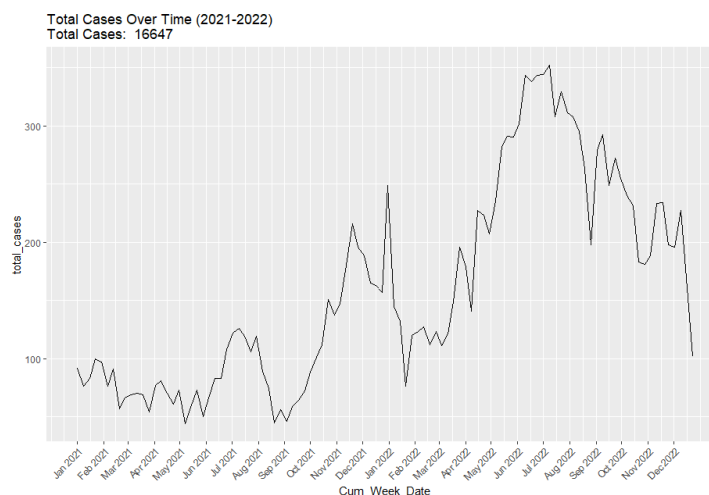


Figure 1: Weekly dengue cases in Region 10.

The choropleth map Figure 2 illustrates dengue case rates per 10,000 individuals across cities and municipalities in Region 10. Areas with the highest dengue rates include Gitagum Danggagan, Valencia City, Linamon and Maigo. These areas have reported high incidences of dengue cases relative to their population sizes. Conversely, regions such as Concepcion, Poona Piagapo, Don Victoriano Chiongbian, Nunungan and Munai report the lowest rates, ranging from minimal to zero cases, which could indicate effective interventions or potential underreporting.

#### 3.1 HMC Diagnostics

Hamiltonian Monte Carlo (HMC) diagnostics were conducted to assess the efficiency and reliability of the Markov Chain Monte Carlo (MCMC) sampling process across all model specifications. HMC is a gradient-based sampling algorithm known for efficiently exploring complex, high-dimensional posterior distributions by simulating Hamiltonian dynamics [15]. In practice, these diagnostics are readily accessible through `RStan`'s built-in tools, such as the `check_hmc_diagnostics()` function, which simplifies the evaluation of sampling behavior [21].

The diagnostics focused on key indicators: divergent transitions, tree depth saturation and the Energy Bayesian Fraction of Missing Information (E-BFMI), all of which are crucial for identifying sampling issues [3]. No divergent transitions were observed across the models, indicating that the posterior geometry was well-behaved. Similarly, there were no signs of tree depth saturation, suggesting that the No-U-Turn Sampler (NUTS) explored the parameter space efficiently without prematurely terminating trajectories. Finally, all E-BFMI values were within acceptable thresholds (typically  $> 0.3$ ), confirming that energy transitions were adequate and that the chains mixed well.

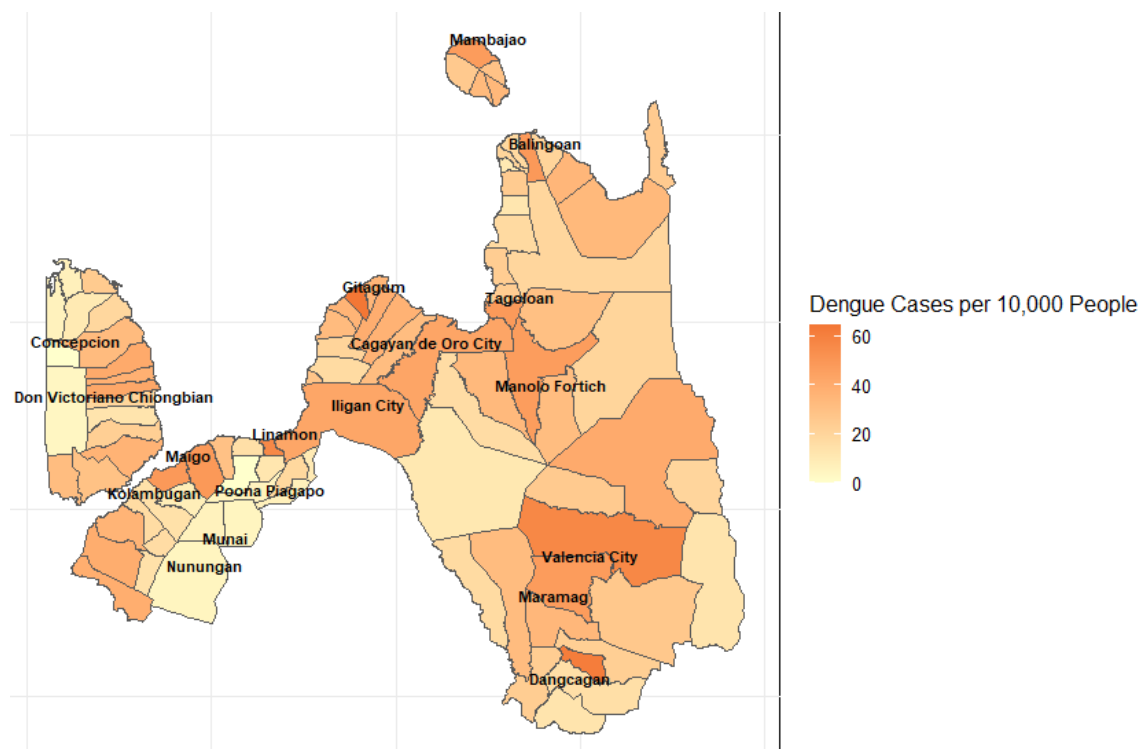


Figure 2: Dengue cases per 10,000 individuals by neighborhood.

Convergence diagnostics further supported the reliability of parameter estimates. The traceplots (Figure 3) indicate stable and well-mixed chains for the parameters in Models 1 to 3.

Additionally, the Gelman-Rubin statistic ( $\hat{R}$ ) was approximately 1 for all parameters, confirming that independent chains converged to the same posterior distribution [11]. As shown in Figure 4, all  $\hat{R}$  values were close to 1.

These diagnostic outcomes collectively suggest that the HMC sampling process successfully captured the posterior structure of each model and provided robust and credible parameter estimates.

### 3.2 Analysis of Covariate Coefficients Across Models

To evaluate the impact of the covariates on dengue incidence, the mean, lower credible interval (CI) and upper CI of their coefficients were examined over the 104-week period (January 2021 to December 2022). This analysis provides insights into the individual effect of each variable on dengue cases, while holding all other factors constant. All variables, including CMCI, were standardized before model estimation. Standardization ensures each variable has a mean of 0 and a standard deviation of 1, allowing for fair comparisons of their effects on dengue incidence. The magnitude of the coefficients thus represents the change in the logarithm of the expected number of dengue cases associated with a one standard deviation increase in the corresponding covariate.

#### 3.2.1 Elevation

Figure 5 presents the posterior estimates of coefficients for estimated elevation, alongside the means and 95% credible intervals over time. In Model 2, where spatial effects are excluded,

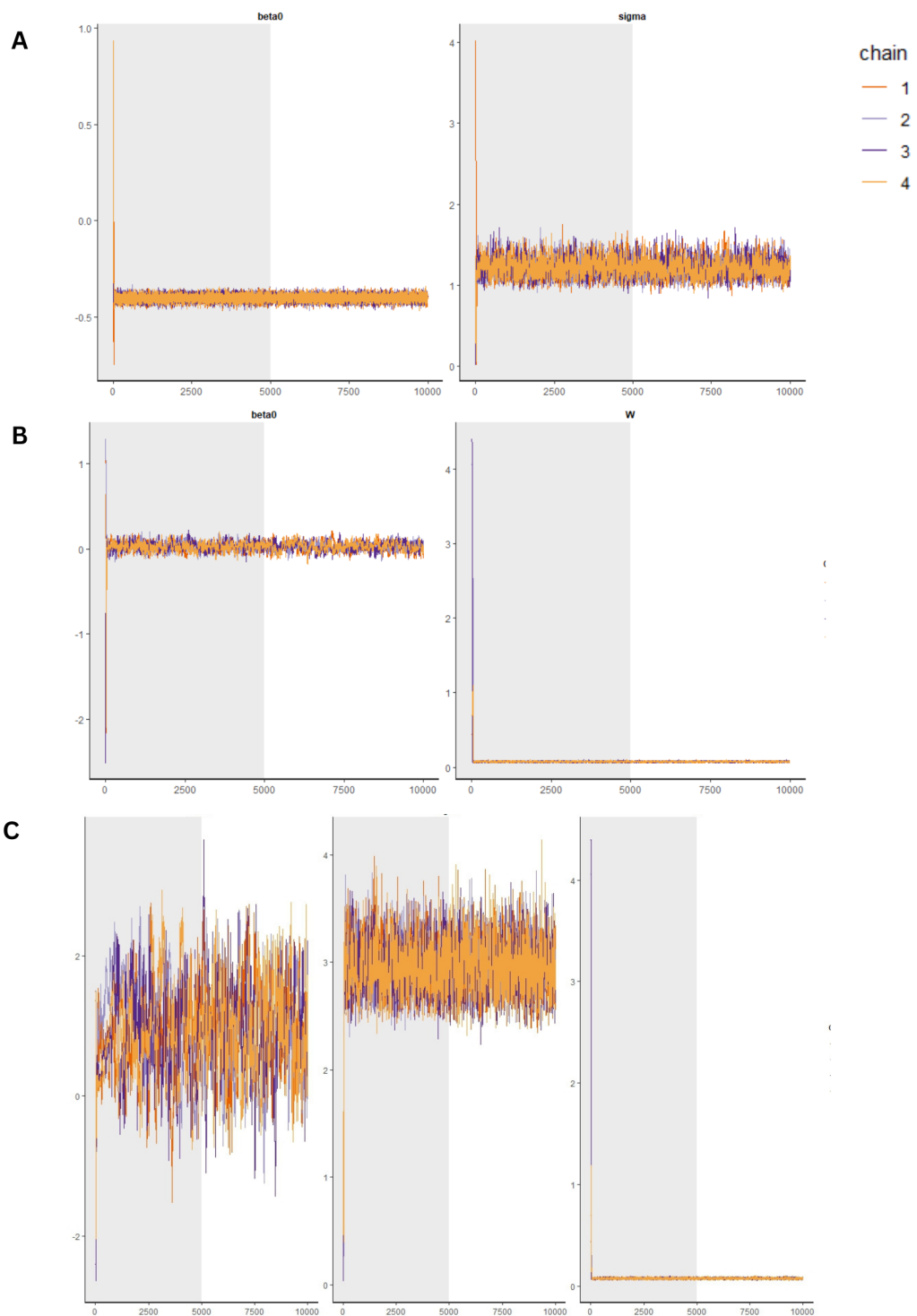


Figure 3: Traceplots for variables of A) Model 1, B) Model 2 and C) Model 3.

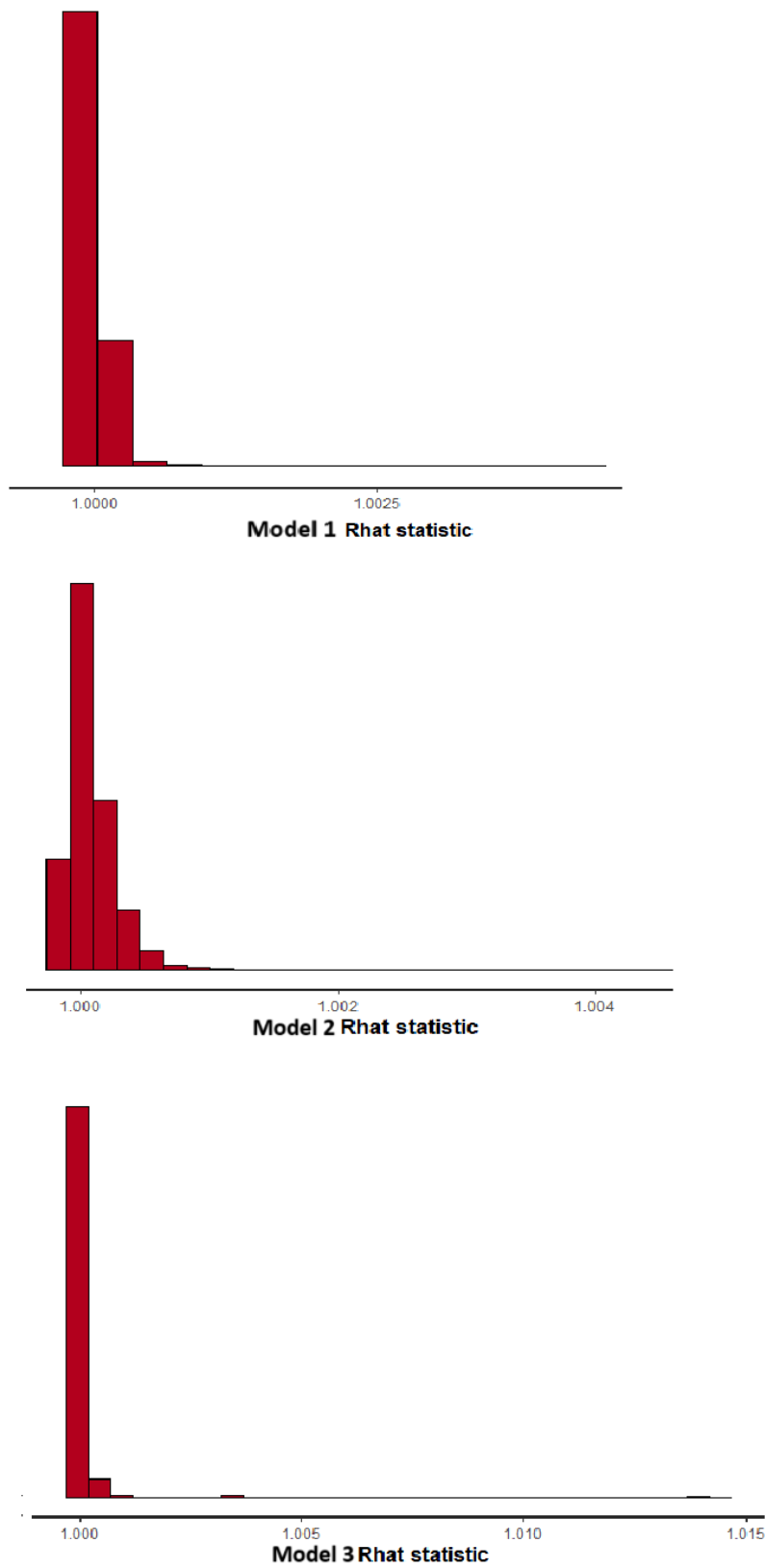


Figure 4: Gelman-Rubin statistic ( $\hat{R}$ ) values for each model.

the coefficient for estimated elevation remains near zero for most of the time period, suggesting that elevation has minimal or inconsistent influence on dengue incidence when spatial dependencies are not accounted for. This indicates that elevation alone, without considering spatial heterogeneity, is insufficient in explaining variations in dengue risk across the region.

However, in Model 3, which incorporates both covariates and spatial effects, the coefficient for elevation shifts to positive values, with the mean ranging from approximately 0.5 to 0.8 during many weeks, occasionally surpassing 0.8. This suggests a moderate positive association between higher elevations and increased dengue incidence when spatial dependencies are considered. The inclusion of spatial effects likely uncovers previously unobserved spatial heterogeneity in dengue transmission, clarifying the relationship between elevation and dengue risk. The positive trend in the coefficient reflects potential interactions between elevation and local factors, such as temperature and mosquito habitat suitability, which may enhance dengue transmission. These findings contrast with studies from other regions, such as Bali, where higher elevations have been associated with reduced dengue risk [7], or Lao PDR, where no significant evidence of elevation-modified dengue transmission was found [23]. In Mexico, *Aedes aegypti* mosquitoes were found to be less abundant at higher elevations, though climate change might expand their range and alter transmission dynamics [13]. These regional differences highlight the complexity of the elevation-dengue relationship, emphasizing the need for context-specific analysis.

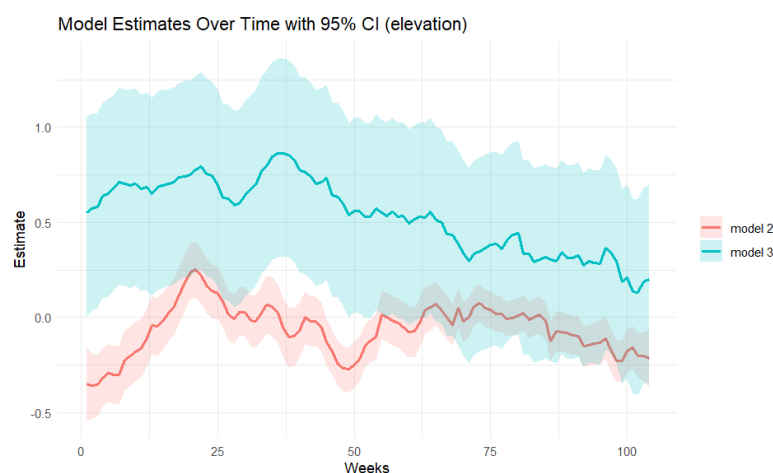


Figure 5: Posterior estimates of the elevation coefficient for Model 2 and Model 3

### 3.2.2 CMCI (Cities and Municipalities Competitiveness Index)

In Model 2, which excludes spatial autocorrelation, the coefficient for CMCI remains relatively stable with small positive values around 0.1. This suggests a slight positive association between CMCI and dengue incidence, indicating that more competitive municipalities—characterized by higher CMCI scores—may experience a small increase in dengue cases. However, the effect is weak and lacks a clear trend, reflecting the limitations of not accounting for spatial dependencies in the model.

In Model 3, which includes spatial autocorrelation, the CMCI coefficient undergoes a noticeable shift, becoming more negative, with mean values ranging from -0.52 to -0.37. This reversal suggests that when spatial effects are considered, higher CMCI scores are associated with a reduction in dengue incidence. The inclusion of spatial dependencies likely suppresses the positive effect observed in Model 2, indicating that dengue transmission dynamics in more competitive municipalities are influenced by factors extending beyond just the socioeconomic

indicators captured by CMCI. This negative association may reflect the spatial heterogeneity of dengue transmission, where municipalities with higher CMCI scores tend to be better equipped with infrastructure, healthcare and vector control measures. These municipalities may be better able to manage dengue outbreaks and mitigate disease spread, aligning with studies that suggest areas with better governance, economic dynamism and resilience may implement more effective public health measures [12]. However, the negative association should be interpreted cautiously, as other underlying factors, such as population density, local climate conditions, and the extent of urbanization, could influence this relationship. Figure 6 presents the posterior estimates of the CMCI coefficient across Models 2 and Model 3.

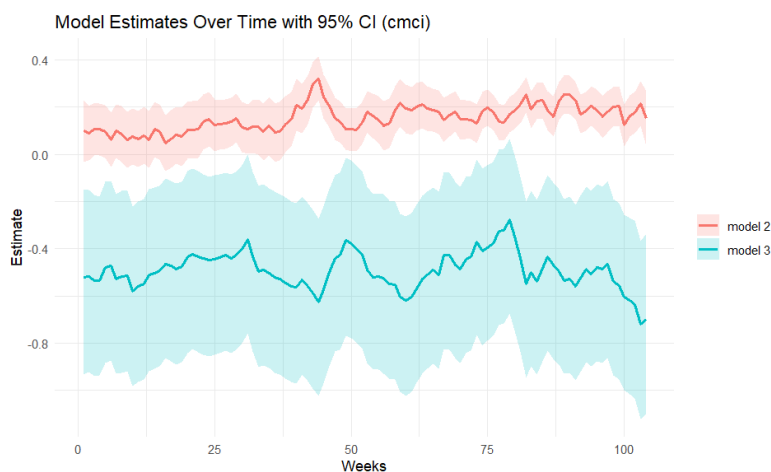


Figure 6: Posterior estimates of the CMCI coefficient for Models 2 and Model 3.

### 3.2.3 Coastal/Landlocked Classification

Figure 7 shows the posterior estimates of the coefficients for coastal/landlocked classification across Model 2 and Model 3. While both models exhibit similar shapes over time, their magnitudes and uncertainty differ. In Model 2, the coefficient fluctuates around zero with narrower credible intervals, suggesting weak or inconsistent effects when spatial structure is ignored. In Model 3, the coefficients shift more negatively, and the credible intervals widen. This indicates a more stable negative association between landlocked areas and dengue incidence, though with increased uncertainty due to accounting for spatial heterogeneity.

The consistent shape suggests the temporal pattern remained, but incorporating spatial effects in Model 3 revealed a clearer and more cautious estimate of the coastal–dengue relationship. The shift in magnitude likely reflects unmeasured spatial factors that influence dengue transmission more strongly in coastal areas.

These findings align with previous studies, which have shown that dengue transmission is significantly influenced by environmental and climate variables, such as temperature and rainfall. García et al. (2023) noted that climate patterns, including temperature fluctuations, can lead to varying transmission rates, especially in coastal regions. Similar spatial patterns of dengue incidence have been reported in Costa Rica, where coastal areas exhibit higher incidence compared to inland regions.



## Model Fit Evaluation

The effective number of parameters,  $p_{\text{WAIC}}$ , and the WAIC values reveal essential insights into model performance. The effective number of parameters provides an estimate of model complexity, indicating the flexibility of each model and its potential risk of overfitting. The WAIC metric serves as a fully Bayesian criterion that balances goodness of fit with complexity, with lower values reflecting better predictive performance. Notably, Model 3 achieves the lowest WAIC (24520.7 with SE 288.9) despite its moderately higher effective parameter count, suggesting that the incorporation of both time-varying covariates and spatial effects leads to a more optimal trade-off between fit and complexity. This result supports the selection of Model 3 as the preferred model for accurately capturing the spatio-temporal dynamics of dengue incidence.

Table 2: Comparison of Model Fit Metrics

Model	Model Structure	$p_{\text{WAIC}}$ (SE)	WAIC (SE)
1	$\log(\mu_{i,t}) = \log(e_i) + \beta_0 + \phi_i$	200.7 (7.6)	29796.3 (403.7)
2	$\log(\mu_{i,t}) = \log(e_i) + \beta_0 + X_i' \beta_{k,t}$	319 (16.8)	26856.8 (320.1)
3	$\log(\mu_{i,t}) = \log(e_i) + \beta_0 + X_i' \beta_{k,t} + \phi_i$	382.6 (15.0)	24520.7 (288.9)

### 3.4 Model 3: Estimated Dengue Risk vs. Observed Cases

This section presents results from the final model (Model 3), which integrates key covariates and spatial effects to estimate dengue relative risk across neighborhoods in Northern Mindanao. Figure 9 showcases the spatial distribution of estimated relative risks for selected weeks. The time points were chosen to capture key seasonal patterns and variations across the study period. Notably, these maps reveal clear spatial heterogeneity in dengue risk, emphasizing the varying influences of covariates and environmental factors on dengue dynamics. For instance, during Week 1, the estimated relative risk is relatively low and uniformly distributed across most areas, reflecting the stable case counts observed in early 2021. By Week 28, a mid-year increase in risk is apparent, coinciding with the onset of seasonal surges. From weeks 65 to 82, there is a noticeable spatial clustering of high-risk neighborhoods, particularly in areas such as Malaybalay, Valencia City and Maramag, along with other regions like Iligan City, Cagayan de Oro, Manolo Fortich and Tagoloan. This clustering suggests concentrated dengue transmission risk in these areas during this period, indicating potential hotspots that require focused attention. When compared to the observed dengue cases (Figure 10), the posterior summaries from Model 3 demonstrate strong alignment with the spatial and temporal trends in actual incidence data.

## 4 Summary and Conclusion

The analysis of dengue transmission in Northern Mindanao highlighted the varying relationships between key covariates and dengue incidence across different model structures. Model 3, which incorporated covariates and a latent spatial effect with an ICAR prior, provided more precise and consistent estimates of the impact of CMCI and coastal/landlocked classification compared to earlier models.

The inclusion of the latent spatial effect ( $\phi_i$ ) in Model 3 led to important shifts in the estimated relationships for the covariates. The result suggests that elevation may play a more substantial role in shaping dengue dynamics in the presence of spatial autocorrelation. The positive relationship observed in Model 3 implies that higher-elevation areas might have environmental or infrastructural characteristics that contribute to increased mosquito breeding or

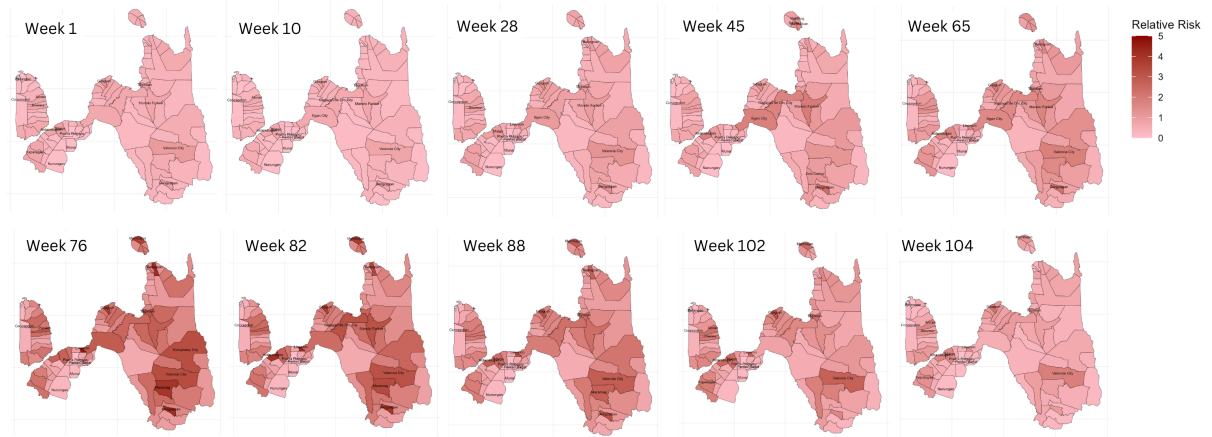


Figure 9: Estimated dengue relative risk by neighborhood over selected weeks, controlling for covariates and spatial effects.

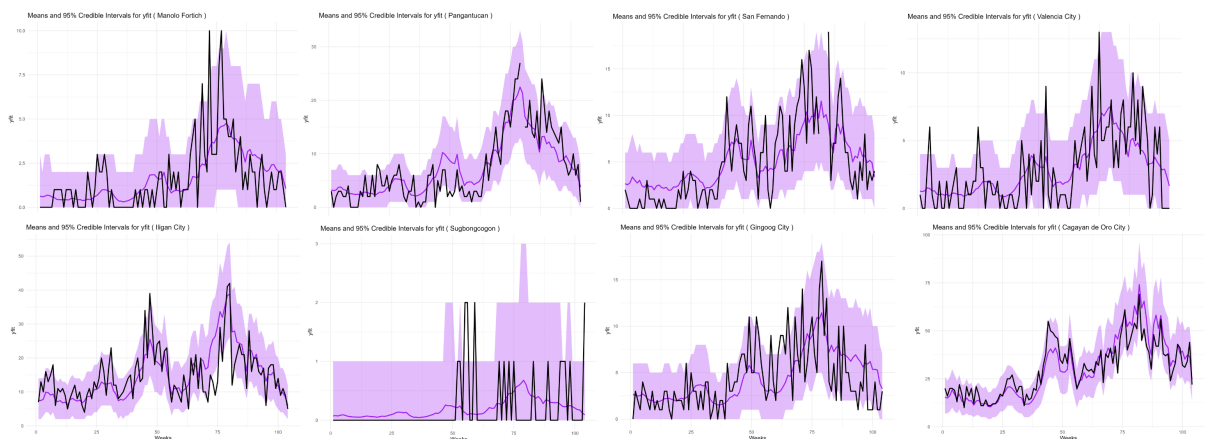


Figure 10: Model 3 Posterior Summaries vs. Observed Dengue Cases.

dengue transmission. Similarly, the relationship between CMCI and dengue incidence underwent a notable shift between Models 2 and 3. This shift to a negative suggests that in regions with higher competitiveness, there may be stronger disease control measures or more effective public health interventions that mitigate the risk of dengue outbreaks, despite the infrastructure or reporting systems that could promote higher case numbers. It was also observed that being classified as coastal was linked to higher mean dengue cases compared to landlocked areas. This may indicate that spatial factors, such as proximity to water bodies, interact differently with dengue dynamics in coastal areas compared to landlocked regions, which could influence mosquito populations and environmental conditions more directly.

The persistent high  $\phi_i$  values in urban areas like Valencia City, Gingoog City, and Cagayan de Oro City show that despite accounting for covariates in Model 3, other unmeasured factors continue to drive spatial variation in dengue risk. Urban areas with higher population density, mobility, and environmental conditions for mosquito breeding may not be fully captured by the covariates. These findings suggest the need for targeted interventions that address both measured and unmeasured risks in these areas. Meanwhile, many municipalities show a reduction in the magnitude of  $\phi_i$ , suggesting that some of the spatial variation initially captured by  $\phi_i$  in Model 1 is now explained by the covariates in Model 3.

The findings emphasize the significance of both temporal and spatial dynamics in dengue transmission. Additionally, the power of Hamiltonian Monte Carlo (HMC) methods in estimating complex models like this cannot be overstated. Given the model's complexity, HMC provided a feasible framework for obtaining reliable estimates. Despite this, the model did exhibit limitations, particularly when locations had long periods of zero cases in consecutive weeks. Zero-inflation, common in disease modeling where periods of inactivity occur, may be a factor contributing to the poor performance in these cases. The model's inability to handle these zero cases effectively indicates that further refinement, such as incorporating zero-inflated terms, could improve robustness in such scenarios.

## Acknowledgements

The authors express their gratitude to the anonymous referees for their valuable comments and suggestions, which significantly improved the quality of this study. Gratitude is also extended to the Department of Health - Northern Mindanao for providing dengue case reports. Additionally, the authors acknowledge the support of the Department of Science and Technology - Science Education Institute (DOST-SEI). This study was made possible in part by the Accelerated Science and Technology Human Resource Development Program (ASTHRDP) scholarship awarded to one of the researchers.

## References

- [1] K. A. Agrupis, M. Ylade, J. Aldaba, A. L. Lopez, and J. Deen, *Trends in dengue research in the Philippines: A systematic review*, PLoS Negl. Trop. Dis. **13** (2019), no. 4, e7280, [doi:10.1371/journal.pntd.0007280](https://doi.org/10.1371/journal.pntd.0007280).
- [2] S. Banerjee, B. P. Carlin, and A. E. Gelfand, *Hierarchical modeling and analysis for spatial data*, CRC Press, Boca Raton, 2014.
- [3] M. Betancourt, *A conceptual introduction to Hamiltonian Monte Carlo*, 2017, [arXiv:1701.02434](https://arxiv.org/abs/1701.02434).

- [4] L. R. Bowman, S. Runge-Ranzinger, and P. J. McCall, *Assessing the relationship between vector indices and dengue transmission: A systematic review of the evidence*, PLoS Negl. Trop. Dis. **8** (2014), no. 5, e2848, doi:10.1371/journal.pntd.0002848.
- [5] L. Bravo, V. G. Roque, J. Brett, R. Dizon, and M. L'Azou, *Epidemiology of dengue disease in the Philippines (2000–2011): A systematic literature review*, PLoS Negl. Trop. Dis. **8** (2014), no. 11, e3027, doi:10.1371/journal.pntd.0003027.
- [6] F. Corpas-Burgos and M. A. Martinez-Beneito, *An autoregressive disease mapping model for spatio-temporal forecasting*, Mathematics **9** (2021), no. 4, 384, doi:10.3390/math9040384.
- [7] P. W. Dhewantara, C. R. Higginson, T. W. Yuliasih, E. A. Wardhani, A. Gouda, C. L. Suwito, B. Simanjuntak, and R. C. Maguire, *Spatial and temporal variation of dengue incidence in the island of Bali, Indonesia: An ecological study*, Travel Med. Infect. Dis. **32** (2019), 101431, doi:10.1016/j.tmaid.2019.06.008.
- [8] Department of Trade and Industry, *About the index – Cities and Municipalities Competitiveness Index*, n.d., <https://cmci.dti.gov.ph/about-index.php>.
- [9] L. P. Freitas, P. M. Carmo, J. F. Codeço, M. F. C. Gonçalves, W. C. Souza, A. C. Medeiros, and G. L. Carvalho, *Spatio-temporal modelling of the first chikungunya epidemic in an intra-urban setting: The role of socioeconomic status, environment and temperature*, PLoS Negl. Trop. Dis. **15** (2021), no. 6, e9537, doi:10.1371/journal.pntd.0009537.
- [10] M. García, M. López, and S. Rodríguez, *Spatial patterns of dengue transmission in Costa Rica: A climate perspective*, Environ. Health Perspect. **131** (2023), no. 6, 067008, doi:10.1289/ehp.2208115.
- [11] A. Gelman and D. B. Rubin, *Inference from iterative simulation using multiple sequences*, Stat. Sci. **7** (1992), no. 4, 457–472.
- [12] A. Kolimenakis, C. Fotakis, E. Papachristos, C. Michaelakis, and S. Kopriva, *The role of urbanisation in the spread of Aedes mosquitoes and the diseases they transmit—A systematic review*, PLoS Negl. Trop. Dis. **15** (2021), no. 8, e9372, doi:10.1371/journal.pntd.0009372.
- [13] S. Lozano-Fuentes, B. J. Fernandez-Salas, J. E. Farfan-Ale, D. U. Loroño-Pino, M. J. Garcia-Rejon, J. G. Luna-Gonzalez, R. Gomez-Carro, G. Liebman, A. A. Uejio, L. B. Steinhoff, R. Eisen, and L. D. Eisen, *The dengue virus mosquito vector Aedes aegypti at high elevation in México*, PLoS Negl. Trop. Dis. **6** (2012), no. 12, e1897, doi:10.1371/journal.pntd.0001897.
- [14] J. P. Messina, O. J. Brady, N. Golding, M. U. Kraemer, F. M. Wint, S. E. Ray, D. M. Pigott, R. C. Myers, C. L. Brownstein, J. S. Hoen, and S. I. Hay, *Global spread of dengue virus types: Mapping the 70-year history*, Trends Microbiol. **22** (2014), no. 3, 138–146, doi:10.1016/j.tim.2013.12.011.
- [15] R. M. Neal, *MCMC using Hamiltonian dynamics*, in *Handbook of Markov Chain Monte Carlo*, S. Brooks, A. Gelman, G. L. Jones, and X.-L. Meng (eds.), Chapman and Hall/CRC, Boca Raton, 2011, arXiv:1206.1901.



- 
- [16] R. D. Peng, *Gelman-Rubin statistic*, in *Advanced Statistical Computing*, 2022, <https://bookdown.org/rdpeng/advstatcomp/monitoring-convergence.html#gelman-rubin-statistic>, [Accessed: Apr. 11, 2025].
- [17] PhilAtlas, *PhilAtlas: Philippine geographic and administrative divisions*, n.d., <https://www.philatlas.com/>.
- [18] M. R. B. Pineda-Cortel, B. M. Clemente, and P. T. T. Nga, *Modeling and predicting dengue fever cases in key regions of the Philippines using remote sensing data*, *Asian Pac. J. Trop. Med.* **12** (2019), no. 2, 60, [doi:10.4103/1995-7645.250838](https://doi.org/10.4103/1995-7645.250838).
- [19] Philippine Statistics Authority, *2020 Census of Population and Housing (2020 CPH) population counts declared official by the President*, 2021, <https://psa.gov.ph/content/2020-census-population-and-housing-2020-cph-population-counts-declared...>
- [20] R Core Team, *R: A language and environment for statistical computing*, R Foundation for Statistical Computing, Vienna, 2023, <https://www.R-project.org/>.
- [21] Stan Development Team, *RStan: The R interface to Stan*, Version 2.26.23, 2023, <https://mc-stan.org>.
- [22] Stan Development Team, *Hamiltonian Monte Carlo*, in *Stan Reference Manual*, Version 2.19, 2019, [https://mc-stan.org/docs/2\\_19/reference-manual/hamiltonian-monte-carlo.html](https://mc-stan.org/docs/2_19/reference-manual/hamiltonian-monte-carlo.html).
- [23] M. Sugeno, S. Khounsy, N. Matsumoto, Y. Nakamura, T. Yoshida, and H. Yokota, *Association between environmental factors and dengue incidence in Lao People's Democratic Republic: A nationwide time-series study*, *BMC Public Health* **23** (2023), 2348, [doi:10.1186/s12889-023-16845-4](https://doi.org/10.1186/s12889-023-16845-4).
- [24] S. Watanabe and M. Opper, *Asymptotic equivalence of Bayes cross validation and widely applicable information criterion in singular learning theory*, *J. Mach. Learn. Res.* **11** (2010), 3571–3594.